Scattering function for a model of interacting surfaces

Pietro Colangelo and Giuseppe Gonnella
Istituto Nationale di Fisica Nucleare, Sezione di Bari, via G. Amendola, 173-70126 Bari, Italy

Amos Maritan
Dipartimento di Fisica dell'Università di Padova, Padova, Italy
(Received 20 April 1992)

The two-point correlation function of an ensemble of interacting closed self-avoiding surfaces on a cubic lattice is analyzed in the disordered phase, which corresponds to the paramagnetic region in a related spin formulation. Mean-field theory and Monte Carlo simulations predict the existence of a disorder line which corresponds to a transition from an exponential decay to an oscillatory damped behavior of the two-point correlation function. The relevance of the results for the description of amphiphilic systems in a microemulsion phase is discussed. The scattering function is also calculated for a bicontinuous phase coexisting with the paramagnetic phase.

PACS number(s): 82.70.Kj, 05.20.Dd, 75.10.−b

I. INTRODUCTION

In recent years considerable efforts have been devoted to applying statistical mechanics in describing and understanding amphiphilic systems, such as oil-water-surfactant mixtures [1]. A phenomenological feature of these systems is that the domains of oil and water remain separated by surfactant monolayers in configurations that depend on various conditions, e.g. the composition of the system, the temperature, etc. In particular, when the concentrations of oil and water are comparable, and under some other conditions, a microemulsion phase appears [2], which is a stable isotropic transparent middle phase that can coexist with the upper nearly-pure-oil phase and with the lower nearly-pure-water phase. Self-diffusion and conductivity measurements [3] lead to the picture of a middle phase consisting of continuous intertwined structures of oil and water [4]. These structures are locally ordered with coherent domains of water and oil on a scale of order 100 Å, as evaluated by scattering experiments [5]. The freeze-fracture electron microscopy gives support to this picture of bicontinuous random structures [6]. For the applications, the interest for the middle phase is due to the ultralow values of the interfacial tensions against the two coexisting phases [7].

The analysis of the data from small-angle neutron and x-ray scattering on systems in the microemulsion phase [5] shows the existence of two characteristic scales of length, a correlation length ξ and a characteristic size of the domains d. As a matter of fact, the measured scattering function $I(q)$ has the form

$$I(q)=\frac{I(0)}{1-bq^2+cq^4}\ , \tag{1}$$

where $q=4\pi/\lambda\sin(\theta/2)$, λ is the probing neutron or x-ray wavelength, and θ is the scattering angle; b and c are positive numbers. $I(q)$ has a peak at $q_p=\sqrt{b/2c}\neq 0$. The two-point density correlation function $h(r)$, which corresponds to Eq. (1), is given by

$$h(r)=\frac{\text{const}}{r}e^{-r/\xi}\sin\frac{2\pi r}{d}\ , \tag{2}$$

with

$$d=\frac{2\pi}{\left[\frac{1}{2\sqrt{c}}+\frac{b}{4c}\right]^{1/2}}\ ,\quad \xi=\frac{1}{\left[\frac{1}{2\sqrt{c}}-\frac{b}{4c}\right]^{1/2}}\ . \tag{3}$$

In the middle phase, at fixed surfactant concentration, the position of the peak q_p does not depend on other parameters such as the cosurfactant concentration and the salinity [8]; it moves towards shorter λ's when the concentration of the amphiphile increases [5]. Typical experimental values for d and ξ are about 250 and 100 Å, respectively, and they decrease as the surfactant concentration increases. Noteworthily, the ratio d/ξ is almost constant over the whole phase, with a value approximately equal to 2.5 [9].

In Ref. [10] we have proposed a lattice model of closed interacting random surfaces that could describe the equilibrium properties of ensembles of fluid films. Our approach is similar to that pioneered by Talmon and Prager [11] and successively refined by many authors [12,13]. In this paper we will study the behavior of the two-point correlation function for the interacting closed surfaces of Ref. [10]. This study is interesting in its own right; moreover, it is worthwhile to consider the possible relations with a phenomenological description of microemulsions. However, we are aware of the oversimplifications that our and similar models have in connection with such applications (for a discussion, see, e.g., Ref. [14]).

Our surfaces are made of plaquettes on a cubic lattice in $\mathbb{R}^3$, without restrictions on the allowed topologies, with the constraint that each plaquette can belong at most to a single surface, i.e., the surfaces are self-avoiding. At variance with previous models, our Hamiltonian, besides including an area-energy term and an extrinsic curvature

term, contains an interaction term arising when two surfaces touch each other along some line [15,16], so that the partition function of the model can be written as

$$Z=\sum_{\mathcal{C}}\exp\{-\beta_s S(\mathcal{C})-\beta_l L(\mathcal{C})-\beta_c C(\mathcal{C})\}\ . \tag{4}$$

The sum is extended over all the configurations of the ensemble. Given a surface configuration $\mathcal{C}$, then $S(\mathcal{C})$, $L(\mathcal{C})$, and $C(\mathcal{C})$ denote, respectively, its total area, the number of links shared by four plaquettes of $\mathcal{C}$, and the number of contiguous plaquettes of $\mathcal{C}$ at a right angle. The quantity $C(\mathcal{C})$ in Eq. (4) is an extrinsic curvature term that favors local configurations with contiguous plaquettes on the same plane when β_c is positive. The model (4) can be expressed as a three-dimensional eight-vertex model where the vertices describe the possible local plaquette configurations (Fig. 1) [16]; the difference with respect to Ref. [16] is that the weights are attributed to the vertices in order to get the most general isotropic model.

As already mentioned, the model Eq. (4) does not constrain the possible surface topology. The role of the topological fluctuations in random surface models has not been clarified from a general point of view yet [17]. On the other hand, these fluctuations frequently occur in real systems: for example, in amphiphilic mixtures it is known that the aggregates of surfactant change easily their topology through a complete fragmentation and a new aggregation of molecules [1]. Therefore Eq. (4) could be sensibly used to describe the phenomenology of systems with large topological fluctuations. An advantage of the lattice formulation is that a structural description can be suitably done by identifying the elementary scale of lengths (the lattice spacing) with some molecular length. The question is about which general properties of amphiphilic systems are codified in the lattice description. In Ref. [10] the attention was mainly focused on the structure of the ordered phases of the model Eq. (4) at zero and finite temperatures. In particular, we have found crystalline bicontinuous phases with cubic symmetry that are of interest in molecular biology [18] and are stable in amphiphilic systems with a high concentration of surfactant. Here we concentrate on the properties of the model Eq. (4) in the disordered high-temperature phase.

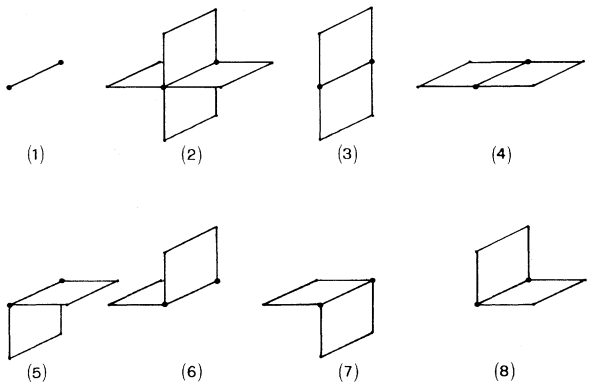

FIG. 1. Plaquette configurations allowed at a link on the cubic lattice are weighted with $\omega_1=e^{\beta_s/2}$, $\omega_2=e^{-\beta_s/2-\beta_l-2\beta_c}$, $\omega_3=\omega_4=1$, $\omega_5=\omega_6=\omega_7=\omega_8=e^{-\beta_c}$.

In the following section we will analyze the behavior of the scattering function and of the corresponding correlation function in the paramagnetic phase of the model Eq. (4) (with $\beta_c=0$) by mean-field and Monte Carlo methods. We will find a region where the scattering function displays a behavior given by Eq. (1). Our results and our predictions for d and ξ will be discussed in relation with the experimental data in Sec. III. In Appendix A it will be shown how the scattering function can be computed in an ordered cubic phase.

II. MEAN-FIELD AND MONTE CARLO RESULTS

It is useful to formulate the partition function Eq. (4) in terms of Ising variables. A set of Ising spins ($\sigma_{\mathbf{r}}=\pm1$) can be defined on the sites $\mathbf{r}$ of the dual lattice, assuming opposite values on the links dual to the plaquettes belonging to the surfaces; the resulting spin model has interactions given by

$$\mathcal{H}=-\beta H=J_1\sum_{\langle \mathbf{r}_1,\mathbf{r}_2\rangle}\sigma_{\mathbf{r}_1}\sigma_{\mathbf{r}_2}+J_2\sum_{\langle\langle \mathbf{r}_1,\mathbf{r}_2\rangle\rangle}\sigma_{\mathbf{r}_1}\sigma_{\mathbf{r}_2}+J_3\sum_{[\mathbf{r}_1,\mathbf{r}_2,\mathbf{r}_3,\mathbf{r}_4]}\sigma_{\mathbf{r}_1}\sigma_{\mathbf{r}_2}\sigma_{\mathbf{r}_3}\sigma_{\mathbf{r}_4}+\text{const}\ , \tag{5}$$

where J_1, J_2, and J_3 can be expressed in terms of the parameters in Eq. (4) through the relations

$$J_1=\frac{\beta_s+\beta_l}{2}+\beta_c\ ,\quad J_2=-\frac{\beta_l}{8}-\frac{\beta_c}{4}\ ,\quad J_3=-\frac{\beta_l}{8}+\frac{\beta_c}{4}\ . \tag{6}$$

In Eq. (5) the three sums, respectively, refer to the nearest-neighboring sites, to the next to the nearest-neighboring sites, and to the plaquettes. In terms of oil-water mixtures, clusters of spin up (down) correspond to oil (water) domains.

The mean-field free-energy corresponding to Eq. (5) is

$$\beta\Gamma=-J_1\sum_{\langle \mathbf{r}_1,\mathbf{r}_2\rangle}m_{\mathbf{r}_1}m_{\mathbf{r}_2}-J_2\sum_{\langle\langle \mathbf{r}_1,\mathbf{r}_2\rangle\rangle}m_{\mathbf{r}_1}m_{\mathbf{r}_2}-J_3\sum_{[\mathbf{r}_1,\mathbf{r}_2,\mathbf{r}_3,\mathbf{r}_4]}m_{\mathbf{r}_1}m_{\mathbf{r}_2}m_{\mathbf{r}_3}m_{\mathbf{r}_4}+\sum_{\mathbf{r}}\left[\frac{1+m_{\mathbf{r}}}{2}\ln(1+m_{\mathbf{r}})+\frac{1-m_{\mathbf{r}}}{2}\ln(1-m_{\mathbf{r}})\right]\ , \tag{7}$$

where $m_{\mathbf{r}}$ is the approximated thermal average of $\sigma_{\mathbf{r}}$ for the configuration that minimizes Eq. (7). The resulting phase diagram with $J_2=J_3$ (i.e., $\beta_c=0$) is reported in Fig. 2 [19]. The existence of a first-order transition line between the two ferromagnetic (nearly pure oil and water) and the disordered phase suggests the possibility of identifying a microemulsion phase in the model. The paramagnetic phase is also in contact with the liquid crystalline cubic bicontinuous phase $\bar{4}$, which is charac-

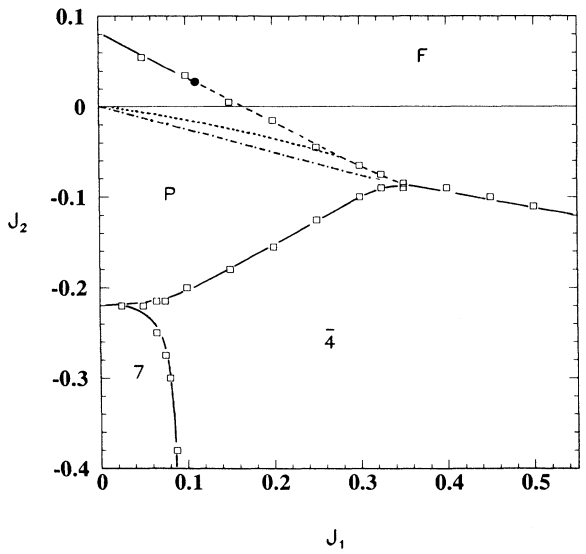

FIG. 2. Mean-field phase diagram. F is the ferromagnetic phase, P the paramagnetic phase. The cubic phase 7 is discussed in Ref. [10]. The continuous lines represent a first-order phase transition, the dashed line denotes a second-order transition. The tricritical point marked with a dot is at $J_1=\frac{1}{9}$, $J_2=\frac{1}{36}$. The dashed-dotted line is the Lifshitz line, whereas the dotted line is the disorder line.

terized in Ref. [10] and corresponds to the cubic phase Q^{229} of Ref. [18]. Therefore the microemulsion phase could be also thought of as the disordered evolution of a cubic bicontinuous phase.

The ferromagnetic (F) and the paramagnetic (P) phases are separated by a transition line with a tricritical point (J_{1t},J_{2t}) in the $J_1,J_2=J_3>0$ region [10]. On the J_1 axis the transition is second order since the spin model reduces to the standard Ising model. When J_1 (J_2) increases (decreases), β_l increases; in terms of random surfaces, this means that self-intersections are not favored. Such an interaction is expected to change neither the order nor the universality class of the transition [16]. For large values of J_2 and $J_1=0$ the ferromagnetic and antiferromagnetic phases are separated by a first-order transition line. These two lines meet at a point where five phases coexist (paramagnetic, two ferromagnetic, and two antiferromagnetic phases). Only turning on the three couplings can make this point a multicritical point [10]. Thus a critical point at a nonvanishing value of J_1 must exist, separating a first-order line at $0<J_1<J_{1t}$ from a second-order line at $J_1>J_{1t}$.

A general aspect of spin systems and fluid models with competing interactions is the existence of a *locus* in the disordered phase where the two-point correlation function changes its behavior from exponentially damped oscillatory to monotonically decaying [20]. This locus is sometimes called *disorder line* [21]. As first proposed in Ref. [22], the disorder line should limit the region that can be identified with a microemulsion phase in amphiphilic system models. If in such models the scattering function has a form as in Eq. (1), the disorder line corresponds to $d^{-1}=0$ [23]. This occurs when $b^2-4c=0$ in Eq. (1), regardless of the sign of b. The $b=0$ line ($b^2-4c<0$) separates the region where $I(q)$ has a peak at $q=0$ ($b<0$) and at $q\neq 0$ ($b>0$), and it is known as the Lifshitz line [22].

The two-point connected correlation function $G_{rr'}=\langle(\sigma_r-m_r)(\sigma_{r'}-m_{r'})\rangle$ is the inverse of the second derivative $\Gamma_{rr'}$ of the free energy, calculated at the minimum of Eq. (7). At this order of the approximation the results do not depend on J_3. Denoting with $\Lambda(\mathbf{q})$ the eigenvalues of $\Gamma_{rr'}$ given by

$$\Lambda(\mathbf{q})=1-2J_1\sum_{\mu=1}^{3}\cos q_\mu -2J_2\sum_{\mu=1}^{2}\sum_{\nu=\mu+1}^{3}[\cos(q_\mu+q_\nu)+\cos(q_\mu-q_\nu)]\ , \tag{8}$$

with $\mathbf{q}=2\pi\mathbf{n}/L$ and $\mathbf{n}$ a three-dimensional vector with components taking all the integer values from 0 to $L-1$ (L is the linear size of the lattice in units of the lattice spacing), one obtains the expressions

$$G_{rr'}=\frac{1}{L^3}\sum_{\mathbf{q}}e^{i\mathbf{q}\cdot(\mathbf{r}-\mathbf{r}')}\frac{1}{\Lambda(\mathbf{q})} \tag{9}$$

and

$$I(\mathbf{q})=\sum_{r,r'}G_{rr'}e^{i\mathbf{q}\cdot(\mathbf{r}'-\mathbf{r})}=\frac{L^3}{\Lambda(\mathbf{q})}\ , \tag{10}$$

so that $I(\mathbf{q})$ is periodic in the components q_1, q_2, q_3. In order to calculate the spherical average $\langle I(\mathbf{q})\rangle$, as a first approximation we can expand $\Lambda(\mathbf{q})$ for small $|\mathbf{q}|$ and take the inverse of the average of $\Lambda(\mathbf{q})$. The result is Eq. (1) with

$$b=-\frac{J_1+4J_2}{1-6J_1-12J_2}\ ,\quad c=-\frac{J_1+8J_2}{1-6J_1-12J_2}\frac{1}{20}\ . \tag{11}$$

A different average with $q_1=q_2=q_3=q/\sqrt{3}$ gives the value $c=-(J_1+16J_2)/[36(1-6J_1-12J_2)]$. Since Eq. (1) must be positive, $b^2-4c<0$. Moreover, the quantity $1-6J_1-12J_2$ is required to be positive in the paramagnetic phase, where $m_r=0$ is the minimum of Γ. From Eqs. (1) and (11) one gets that $\langle I(\mathbf{q})\rangle$ has a maximum at $q\neq 0$ if $J_2<-J_1/4$ and $J_1<\frac{1}{3}$, where all the constraints are satisfied. The line $J_2=-J_1/4$ is the Lifshitz line in the mean-field approximation and is represented by the dashed-dotted line in Fig. 2; in the same figure the dotted line represents the disorder line.

The exact spherical average can be calculated numerically using Eqs. (8) and (10). The result for $J_1=0.2$ and $J_2=-0.1$ is shown in Fig. 3. The macroscopical behavior of the system can be analyzed considering in the average $\langle I(\mathbf{q})\rangle$ the small q region including the first peak (shown in the inset of Fig. 3). Fitting these curves with Eq. (1) we obtain an evaluation of d and ξ. The results, for various J_1 and J_2, are shown in Fig. 4; they appear to

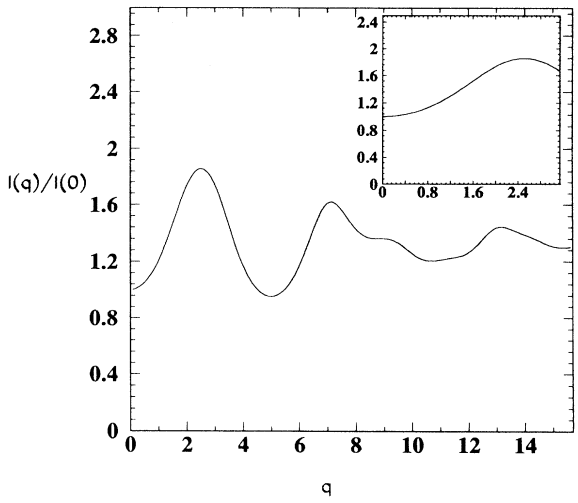

FIG. 3. Exact spherical average of $I(\mathbf{q})/L^3$ at $J_1=0.2$, $J_2=-0.1$. In the inset the interval $0\le q\le\pi$ is shown.

be in qualitative agreement with Eqs. (3) and (11). The maximum of $\langle I(\mathbf{q})\rangle$ still occurs at $q\neq 0$ for $J_2<-J_1/4$.

The function $I(\mathbf{q})$ defined in Eq. (10) can be also calculated for an ordered phase where it represents the contribution of the fluctuations to be added to the Bragg scattering function

$$I_B(\mathbf{q})=\left|\sum_{\mathbf{r}} m_{\mathbf{r}} e^{i\mathbf{q}\cdot\mathbf{r}}\right|^2 . \tag{12}$$

The functions $I(\mathbf{q})$ and $I_B(\mathbf{q})$ have been calculated for states in the bicontinuous phase $\overline{4}$. The configuration of the phase $\overline{4}$ can be obtained by tiling the whole lattice with the cube shown in Fig. 5. Since the magnetizations $m_{\mathbf{r}}$ vary on the cube, the second derivatives $\Gamma_{\mathbf{r}\mathbf{r}'}$ depend on the values of $\mathbf{r}$ and $\mathbf{r}'$ considered. To diagonalize $\Gamma_{\mathbf{r}\mathbf{r}'}$ it is convenient to consider the whole L^3 lattice as a $(L/2)^3$ lattice of elementary cubes with a basis of eight magnetizations for each site of the new lattice. Using this procedure (details can be found in Appendix A), we get an 8×8 Hermitian matrix to be diagonalized. The eigenvalues and eigenvectors can be found numerically for each point (J_1,J_2,J_3) after the insertion of the corresponding values of the magnetizations as given by the mean-field equations. Then, applying the formula (A6), one obtains an evaluation of $I(\mathbf{q})$. The spherically averaged $\langle I(\mathbf{q})\rangle$ is depicted in Fig. 6 for a point just below the paramagnetic phase. Here the first Bragg peak occurs at $q=\pi$.

In order to check the accuracy of the mean-field predictions, we have performed a Monte Carlo analysis of the spin model in the disordered high-temperature phase. The numerical simulations have been carried out on a lattice of $(30)^3$ sites with periodic boundary conditions. For each point in the domain $0\le J_1\le 1.2$, $-0.5\le J_2=J_3\le 0$ of the coupling constants, 2×10^4 sweeps have been per-

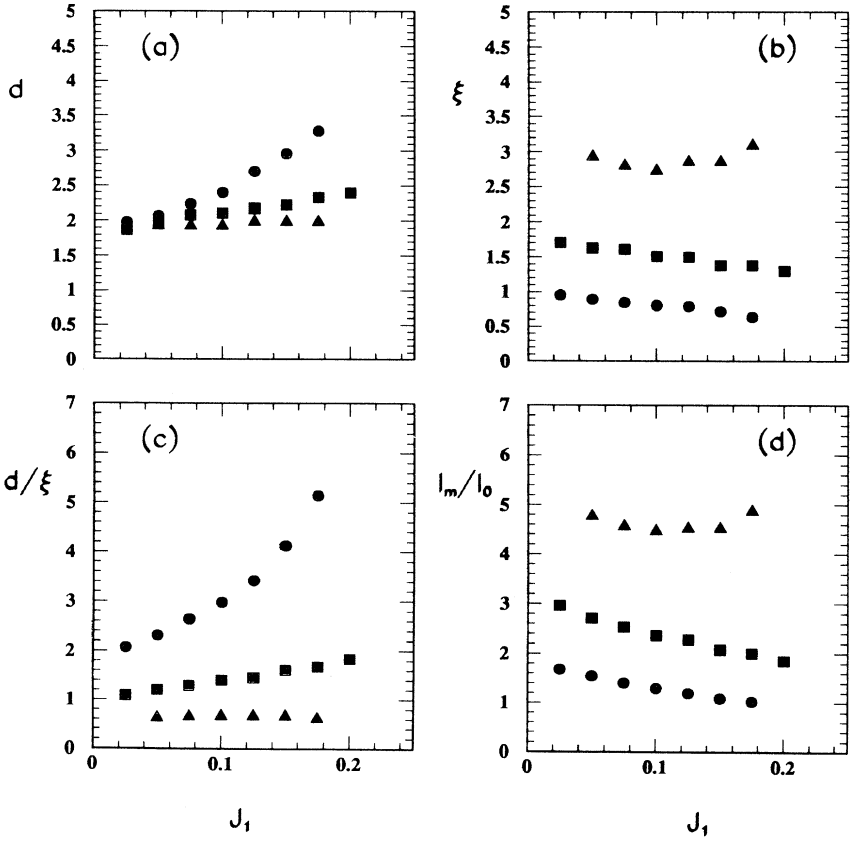

FIG. 4. Values of d (a), ξ (b), d/ξ (c), and $I(q_p)/I(0)$ (d) obtained from the spherical average of the mean-field scattering function $I(\mathbf{q})$ are shown in the microemulsion region as functions of J_1, which regulates the interface area, for $J_2=-0.05$ (dots), $J_2=-0.10$ (squares), and $J_2=-0.15$ (triangles).

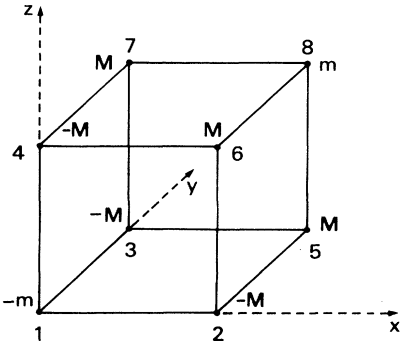

FIG. 5. Bicontinuous film crystal $\bar{4}$ can be obtained by tiling the cubic lattice with the spin configuration shown in the picture.

formed using the Metropolis algorithm and a long period random number generator [24], starting from ordered and disordered initial configurations. 1×10^4 sweeps have been discarded to allow thermalization. The measured quantity is the two-point correlation function

$$h(r)=\frac{1}{L^3}\sum_{i-j=r}[\langle\sigma(i)\sigma(j)\rangle-\langle\sigma(i)\rangle\langle\sigma(j)\rangle]\,, \qquad (13)$$

the data have been analyzed taking into account the correlations between the measurements.

The obtained phase diagram is shown in Fig. 7. As already observed in Ref. [10], the main difference with respect to the mean-field diagram is that the paramagnetic phase seems to extend to zero temperature along the line $J_2=-J_1/4$; therefore, the ferromagnetic (F) and the cubic (C) regions remain separated, whereas in the mean-field calculation they have a common transition line. The correlation function $h(r)$ has been evaluated at fixed values of J_1 along vertical lines in the (J_1,J_2) plane. In the region immediately below the ferroparamagnetic transition line, $h(r)$ displays a decreasing (exponential) behavior in r, as can be observed in Fig. 8(a) at

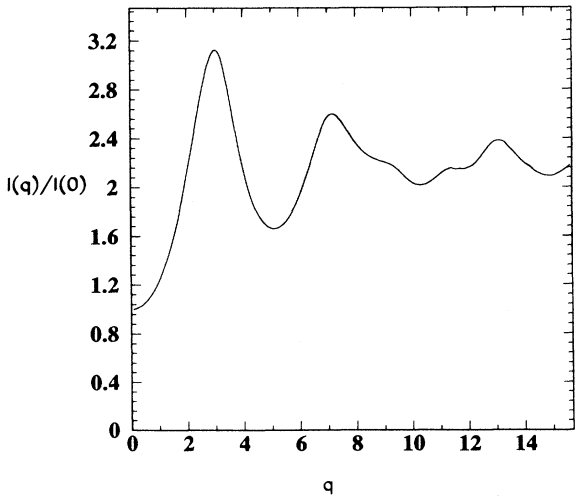

FIG. 6. Spherical average of the fluctuation contribution $I(\mathbf{q})/L^3$ to the scattering function in the phase $\bar{4}$ for $J_1=0.20$, $J_2=-0.16$.

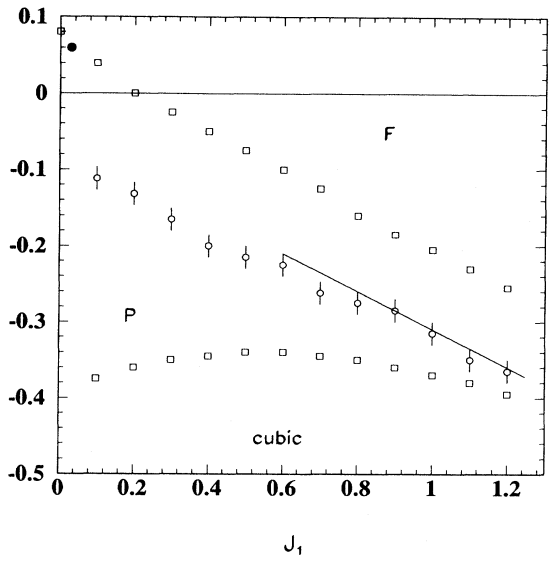

FIG. 7. Phase diagram obtained by Monte Carlo simulations. F and P are the ferromagnetic and the paramagnetic phases. The tricritical point marked with a dot is at $J_1=0.03$, $J_2=0.06$. The ferromagnetic-paramagnetic transition line from $J_1=0$ to the tricritical point is first order. The continuous line that fits the disorder line has a slope $-\frac{1}{4}$.

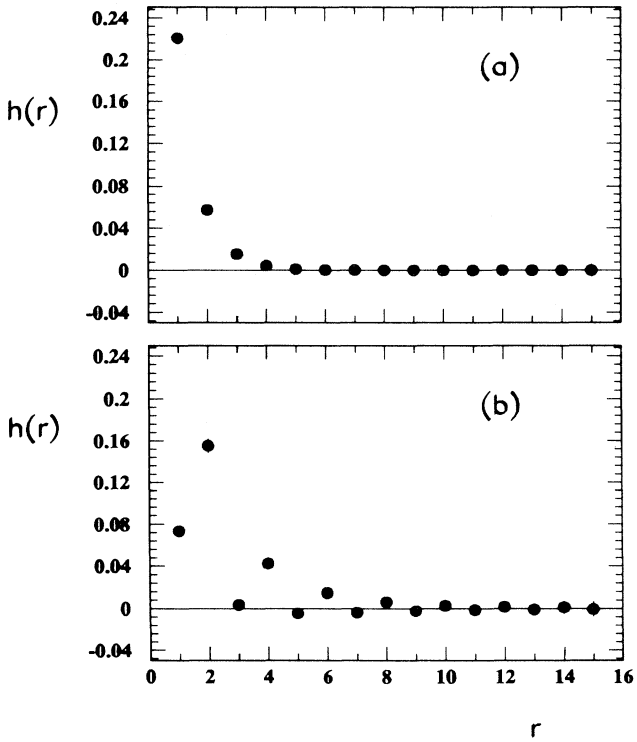

FIG. 8. Correlation function $h(r)$, as calculated from Monte Carlo simulations, at $(J_1,J_2)=(0.50,-0.12)$ above the disorder line (a) and at $(J_1,J_2)=(0.50,-0.30)$ below the disorder line (b). In both cases $h(0)=1$.

$(J_1,J_2)=(0.50,-0.12)$; when J_2 decreases, the functional dependence of $h(r)$ changes to a damped oscillating behavior, as depicted in Fig. 8(b) at $(J_1,J_2)=(0.50,-0.30)$ [(M) region in Fig. 7]. The value of J_2, where the change in the functional dependence occurs, is fixed assuming the criterion that at least one complete period of oscillation is observed. The obtained disorder line is nearly parallel to the ferroparamagnetic transition line; this feature is common to the two-dimensional eight-vertex model, where the disorder line does not have intersections with any other transition line [25].

A quantitative evaluation of ξ and d from numerical data is quite difficult; as a matter of fact, the behavior equation (2) should be reproduced for large values of the distance r, whereas on a finite lattice the interval in r is limited and the statistical errors increase as r does. We have fitted $h(r)$ with a function like Eq. (2) including also the possibility of an additional constant phase in the argument of the sinus [26]. The fit gives results if at least the first three points of $h(r)$ are discarded. Along the line $J_2=-0.30$ we get, regardless to J_1 in the (M) region, a nearly constant value $\xi=0.6\pm0.2$ and $d=2.2\pm0.3$, so that the ratio $d/\xi\simeq4$. The same analysis, carried out using a lattice of $(40)^3$ sites at $(J_1,J_2)=(0.50,-0.30)$, shows that ξ and d do not depend on the lattice size.

It is worth comparing these numerical results with the predictions of the mean-field theory collected in Fig. 4. The Monte Carlo value $d\simeq2$ agrees with the mean-field result, for example, at $J_2=-0.15$. However, the mean-field result displays an increasing behavior in J_1 that we are unable to observe in the simulations, probably due to the statistical errors. As for ξ, the values for the correlation length seem to be sensibly overestimated by the mean-field theory.

TABLE I. The elements of the matrix $\mathcal{T}$.

Matrix element
$\mathcal{T}_{11}=\mathcal{T}_{88}=\dfrac{1}{1-m^2}$
$\mathcal{T}_{12}=\mathcal{T}_{78}=(-J_1+4J_3M^2)(1+e^{-ip_1})$
$\mathcal{T}_{13}=\mathcal{T}_{68}=(-J_1+4J_3M^2)(1+e^{-ip_2})$
$\mathcal{T}_{14}=\mathcal{T}_{58}=(-J_1+4J_3M^2)(1+e^{-ip_3})$
$\mathcal{T}_{15}=\mathcal{T}_{48}=(-J_2-J_3M^2)(1+e^{-ip_1}+e^{-ip_2}+e^{-i(p_1+p_2)})$
$\mathcal{T}_{16}=\mathcal{T}_{38}=(-J_2-J_3M^2)(1+e^{-ip_1}+e^{-ip_3}+e^{-i(p_1+p_3)})$
$\mathcal{T}_{17}=\mathcal{T}_{28}=(-J_2-J_3M^2)(1+e^{-ip_2}+e^{-ip_3}+e^{-i(p_3+p_2)})$
$\mathcal{T}_{18}=\mathcal{T}_{27}=\mathcal{T}_{36}=\mathcal{T}_{45}=0$
$\mathcal{T}_{22}=\mathcal{T}_{33}=\mathcal{T}_{44}=\mathcal{T}_{55}=\mathcal{T}_{66}=\mathcal{T}_{77}=\dfrac{1}{1-M^2}$
$\mathcal{T}_{23}=\mathcal{T}_{67}=(-J_2+J_3Mm)(1+e^{ip_1}+e^{-ip_2}+e^{+i(p_1-p_2)})$
$\mathcal{T}_{24}=\mathcal{T}_{57}=(-J_2+J_3Mm)(1+e^{ip_1}+e^{-ip_3}+e^{+i(p_1-p_3)})$
$\mathcal{T}_{25}=\mathcal{T}_{47}=(-J_1-4J_3Mm)(1+e^{-ip_2})$
$\mathcal{T}_{26}=\mathcal{T}_{37}=(-J_1-4J_3Mm)(1+e^{-ip_3})$
$\mathcal{T}_{34}=\mathcal{T}_{56}=(-J_2+J_3Mm)(1+e^{ip_2}+e^{-ip_3}+e^{+i(p_2-p_3)})$
$\mathcal{T}_{35}=\mathcal{T}_{46}=(-J_1-4J_3Mm)(1+e^{-ip_1})$

III. DISCUSSION AND CONCLUSIONS

In a realistic microemulsion model the disorder line should intersect the first order ferroparamagnetic transition line to ensure the coexistence between the microemulsion phase and the nearly-pure-oil and nearly-pure-water phases. As we have shown in the previous section, this feature is absent in our model, where, in the region of the parameters considered ($\beta_c=0$), the disorder line is nearly parallel to the F-P transition line from Monte Carlo simulation, whereas it intersects the second order F-P transition from mean field. Nevertheless, it is interesting to compare the experimental data of d and ξ with our results.

The values of d, ξ, and q_p (for definiteness we use the results from the simulations) can be compared with the values measured in the experiment if a physical length is assigned to the lattice spacing a. We can identify a with the persistence length ξ_K of Ref. [2], which represents the scale on which a fluid surface like a surfactant interface can be considered stiff. The values $d_{\rm phys}\approx250$ Å and $\xi_{\rm phys}\approx100$ Å correspond, for $d\approx2.2$ and $\xi=0.6$, to a lattice spacing $a=100$–160 Å. Then our prediction is in (qualitative) agreement with the value $\xi_K\approx100$ Å, which has been evaluated to be typical for the bicontinuous phase [27]. However, the ratio $d/\xi\approx4$ appears to be larger than the dependence $\xi=0.4d$ observed by Widom [9], using the compilation of data of Teubner and Strey [5]. Moreover, the mean field shows a dependence of d on J_1. One observes that d has increasing values when the interface area decreases, since in our model to increase the surfactant concentration corresponds to decrease β_s.

In conclusion, the random surface model corresponding to the eight-vertex model describes some structural properties of a microemulsion phase. The lack of coexistence between this phase and the ferromagnetic one observed for $J_2=J_3$ or $\beta_c=0$ indicates that our model, with the parameters considered here, cannot be interpreted as a realistic model for describing the phase diagram of amphiphilic systems. Nevertheless, considering that our starting point was more general—to describe the equilibrium properties of systems of fluid surfaces with a variable number of components—we find that the agreement of our results with the experiments is noticeable. Moreover, a realistic phase diagram might emerge for different values of the parameters, when the extrinsic curvature energy is considered.

APPENDIX: THE SCATTERING FUNCTION OF A CUBIC PHASE

In order to calculate the function $I(\mathbf{q})$ of Eq. (10) when the equilibrium configuration is the cubic phase represented in Fig. 5, we need to diagonalize the matrix of the second derivatives of the free energy of Eq. (7) with respect to $m_{\mathbf{r}}$ and

$m_{\mathbf{r}'}$, evaluated in the phase of Fig. 5. We choose a coordinate system as in Fig. 5, denote with μ one of the three unit vectors, and assume periodic boundary conditions on a cubic lattice with linear size L (even). Then $\Gamma_{\mathbf{r}\mathbf{r}'}$ is given by

$$\Gamma_{\mathbf{r}\mathbf{r}'}=\begin{cases}-J_1-4J_3M\left[-M\dfrac{1-(-1)^{1+r_{\mu+1}+r_{\mu+2}}}{2}+m\dfrac{1-(-1)^{r_{\mu+1}+r_{\mu+2}}}{2}\right] & \text{if } r'=r+\mu \\ -J_2-J_3M\left[M\dfrac{1-(-1)^{1+r_\mu+r_\nu}}{2}-m\dfrac{1-(-1)^{r_\mu+r_\nu}}{2}\right] & \text{if } \mathbf{r}=\mathbf{r}\pm\mu\pm\nu,\ \ \mu\neq\nu \\ \delta(\mathbf{r},M)\dfrac{1}{1-M^2}+\delta(\mathbf{r},m)\dfrac{1}{1-m^2} & \text{if } \mathbf{r}=\mathbf{r}' \ , \end{cases} \tag{A1}$$

where the functions $\delta(\mathbf{r},M)$ and $\delta(\mathbf{r},m)$ are equal to 1 if the magnetization at the site $\mathbf{r}$ is $\pm M$ or $\pm m$, respectively; otherwise, they vanish. Since the above matrix is periodic along the three axes with a period of two lattice spacings, it is convenient to define a new lattice whose sites are defined only on the even sites of the original lattice. The position of the new sites is denoted by $\mathbf{R}$. For each site $\mathbf{R}$ ($R_\mu=0,1,\ldots,L/2-1$) one has a basis with eight magnetizations labeled with $a,b,\ldots$ ($a,b,\ldots=1,\ldots,8$) and numbered as in Fig. 5. Then the matrix $\Gamma_{\mathbf{r}\mathbf{r}'}$ can be written as

$$\begin{aligned}\Gamma_{\mathbf{r}\mathbf{r}'}\equiv\Gamma_{\{\mathbf{R},a\}\{\mathbf{R}',b\}}\equiv{}&\delta_{\mathbf{R}\mathbf{R}'}A_{ab}+\delta_{\mathbf{R}\mathbf{R}'-2\mathbf{i}}X^+_{ab}+\delta_{\mathbf{R}\mathbf{R}'+2\mathbf{i}}X^-_{ab}+\delta_{\mathbf{R}\mathbf{R}'-2\mathbf{j}}Y^+_{ab}+\delta_{\mathbf{R}\mathbf{R}'+2\mathbf{j}}Y^-_{ab}+\delta_{\mathbf{R}\mathbf{R}'-2\mathbf{k}}Z^+_{ab}+\delta_{\mathbf{R}\mathbf{R}'+2\mathbf{k}}Z^-_{ab}\\&+\delta_{\mathbf{R}\mathbf{R}'-2\mathbf{i}-2\mathbf{j}}(XY^{++})_{ab}+\delta_{\mathbf{R}\mathbf{R}'+2\mathbf{i}+2\mathbf{j}}(XY^{--})_{ab}+\delta_{\mathbf{R}\mathbf{R}'-2\mathbf{i}+2\mathbf{j}}(XY^{+-})_{ab}\\&+\delta_{\mathbf{R}\mathbf{R}'+2\mathbf{i}-2\mathbf{j}}(XY^{-+})_{ab}+\delta_{\mathbf{R}\mathbf{R}'-2\mathbf{i}-2\mathbf{k}}(XZ^{++})_{ab}+\delta_{\mathbf{R}\mathbf{R}'+2\mathbf{i}+2\mathbf{k}}(XZ^{--})_{ab}\\&+\delta_{\mathbf{R}\mathbf{R}'-2\mathbf{i}+2\mathbf{k}}(XZ^{+-})_{ab}+\delta_{\mathbf{R}\mathbf{R}'+2\mathbf{i}-2\mathbf{k}}(XZ^{-+})_{ab}+\delta_{\mathbf{R}\mathbf{R}'-2\mathbf{j}-2\mathbf{k}}(YZ^{++})_{ab}\\&+\delta_{\mathbf{R}\mathbf{R}'+2\mathbf{j}+2\mathbf{k}}(YZ^{--})_{ab}+\delta_{\mathbf{R}\mathbf{R}'-2\mathbf{j}+2\mathbf{k}}(YZ^{+-})_{ab}+\delta_{\mathbf{R}\mathbf{R}'+2\mathbf{j}-2\mathbf{k}}(YZ^{-+})_{ab} \ ,\end{aligned} \tag{A2}$$

where the matrices A, X^+, XY^{++}, etc. can be easily obtained from Eq. (A1).

Then one considers eigenfunctions of $\Gamma_{\{\mathbf{R},a\}\{\mathbf{R}',b\}}$ as

$$\psi_{\mathbf{R},a}=\left[\frac{2}{L}\right]^{3/2}\phi_a(\mathbf{p})e^{i\mathbf{p}\cdot\mathbf{R}} \ , \tag{A3}$$

with $p^\mu=4\pi n^\mu/L$ and $n^\mu=0,1,\ldots,L/2-1$, so that the ϕ_b's are the eigenvectors of the Hermitian matrix $\mathcal{T}(\mathbf{p})$ defined by

$$\sum_{\mathbf{R}',b}\Gamma_{\{\mathbf{R},a\}\{\mathbf{R}',b\}}\psi_{\{\mathbf{R}',b\}}=\sum_b\mathcal{T}_{ab}(\mathbf{p})\psi_{\{\mathbf{R},b\}} \ , \tag{A4}$$

with components written in Table I.

For each set of couplings J_i and for each $\mathbf{p}$ the eigenvalues $\lambda^{(a)}(\mathbf{p})$ of the matrix $\mathcal{T}(\mathbf{p})$ ($a=1,\ldots,8$) and the corresponding eigenvectors $\phi^{(a)}_b(\mathbf{p})$ can be found numerically. Since ($\mathbf{r}'\equiv\{\mathbf{R}',a'\},\mathbf{r}''\equiv\{\mathbf{R}'',a''\}$),

$$\begin{aligned}I(\mathbf{q})=\sum_{\mathbf{r}',\mathbf{r}''}(\Gamma^{-1})_{\mathbf{r}',\mathbf{r}''}e^{i\mathbf{q}\cdot(\mathbf{r}''-\mathbf{r}')}&=\sum_{\mathbf{r}',\mathbf{r}''}\sum_{(a),\mathbf{p}}\frac{1}{\lambda^{(a)}(\mathbf{p})}\psi^{(a)}_{\{\mathbf{R}',a'\}}(\mathbf{p})\psi^{\dagger(a)}_{\{\mathbf{R}'',a''\}}(\mathbf{p})e^{i\mathbf{q}\cdot(\mathbf{r}''-\mathbf{r}')}\\&=\sum_{(a),\mathbf{p}}\frac{1}{\lambda^{(a)}(\mathbf{p})}\left|\sum_{\mathbf{r}'}\psi_{\{\mathbf{R}',a'\}}(\mathbf{p})e^{-i\mathbf{q}\cdot\mathbf{r}'}\right|^2 \ ,\end{aligned} \tag{A5}$$

where $\mathbf{q}$ is the scattering vector, using the relation $\sum_{x=0,2,\ldots}^{L-2}e^{i(p_x-q_x)x}=(L/2)\delta_{p_xq_x}$, one obtains the final result

$$\begin{aligned}\frac{8I(\mathbf{q})}{L^3}=\sum_{(a)}\frac{1}{\lambda^{(a)}(2\mathbf{q})}\Big|&\phi^{(a)}_1(2\mathbf{q})+\phi^{(a)}_2(2\mathbf{q})e^{-iq_1}+\phi^{(a)}_3(2\mathbf{q})e^{-iq_2}+\phi^{(a)}_4(2\mathbf{q})e^{-iq_3}\\&+\phi^{(a)}_5(2\mathbf{q})e^{-i(q_1+q_2)}+\phi^{(a)}_6(2\mathbf{q})e^{-i(q_1+q_3)}+\phi^{(a)}_7(2\mathbf{q})e^{-i(q_2+q_3)}+\phi^{(a)}_8(2\mathbf{q})e^{-i(q_1+q_2+q_3)}\Big|^2 \ .\end{aligned} \tag{A6}$$

[1] *Physics of Amphiphilic Layers,* edited by J. Meunier, D. Langevin, and N. Boccara (Springer-Verlag, Berlin, 1987).

[2] P. G. de Gennes and C. Taupin, J. Phys. Chem. **86**, 2294 (1982).

[3] F. Larche, J. Rouviere, P. Delord, B. Brun, and J. L. Dussosoy, J. Phys. Lett. **41**, L437 (1980); B. Lindman, N. Kamenka, T. M. Kathopoulis, B. Brun, and P. G. Nilsson, J. Phys. Chem. **84**, 2485 (1980); M. Clausse, P. Peyrelasse, J.

Heil, C. Boned, and B. Lagourette, Nature **293**, 636 (1981).
[4] L. E. Scriven, Nature **263**, 123 (1976).
[5] M. Teubner and R. Strey, J. Chem. Phys. **87**, 3195 (1987).
[6] W. Jahn and R. Strey, J. Phys. Chem. **92**, 2294 (1988).
[7] See, e.g., H. T. Davis, J. F. Bodet, L. E. Scriven, and W. G. Miller in *Physics of Amphiphilic Layers* (Ref. [1]), p. 310.
[8] See, e.g., A. de Geyer and J. Tabony in *Physics of Amphiphilic Layers* (Ref. [1]), p. 374.
[9] B. Widom, J. Chem. Phys. **90**, 2437 (1989).
[10] A. Cappi, P. Colangelo, G. Gonnella, and A. Maritan, Nucl. Phys. B **370**, 659 (1992).
[11] Y. Talmon and S. Prager, J. Chem. Phys. **69**, 2984 (1978).
[12] In a class of lattice models for microemulsions, one assumes a microscopic point of view identifying the links of the lattice with the molecules and introducing a phenomenological interaction between neighboring molecules. See Refs. [73–87] of the lectures of B. Widom, in *Liquids, Freezing and Glass Transition,* edited by J. P. Hansen, D. Levesque, and J. Zinn-Justin (North-Holland, Amsterdam, 1991), p. 541.
[13] L. Golubovic and T. C. Lubensky, Phys. Rev. A **41**, 4343 (1990).
[14] K. Chen, C. Ebner, C. Jayaprakash, and R. Pandit, Phys. Rev. A **38**, 6240 (1988).
[15] More general interaction terms are not believed to change the phase diagram qualitatively.
[16] T. Sterling and J. Greensite, Phys. Lett. B **121**, 345 (1983); M. Karowski, J. Phys. A **19**, 3375 (1986).
[17] M. Karowski and H. J. Thun, Phys. Rev. Lett. **54**, 2556 (1985); D. A. Huse, *ibid.* **64**, 3200 (1990); R. Schrader, J. Stat. Phys. **40**, 533 (1985).
[18] P. Mariani, V. Luzzati, and H. Delacroix, J. Mol. Biol. **204**, 165 (1988).
[19] See Ref. [10]; the portion of the phase diagram with $J_1 < 0$ is the antiferromagnetic image of the diagram with $J_1 > 0$. For values of the couplings that favor flat surface configurations, we find lamellar phases instead of cubic bicontinuous phases.
[20] M. E. Fisher and B. Widom, J. Chem. Phys. **50**, 3756 (1968).
[21] J. Stephenson, J. Math. Phys. **11**, 420 (1970).
[22] G. Gompper and M. Schick, Phys. Rev. Lett. **14**, 1647 (1989); Phys. Rev. B **41**, 9148 (1990).
[23] In various three-dimensional lattice models the disorder line and the scattering function have been calculated in the mean-field approximation; see Refs. [9,22], and also M. W. Matsen and D. E. Sullivan, Phys. Rev. A **41**, 2021 (1990).
[24] F. James, Comput. Phys. Commun. **60**, 329 (1990).
[25] See, for example, F. S. Rys, Phys. Rev. Lett. **51**, 849 (1983).
[26] A nonvanishing phase ϕ in the argument of the sinus in Eq. (2) modifies the scattering function as follows: $I(q)/I(0)=(1+aq^2)/(1-bq^2+cq^4)$ with $\tan\phi=[a(4c-b^2)^{1/2}]/(2c+ab)$.
[27] For an experimental evaluation of the persistence length, see, for example J. Meunier in *Physics of Amphiphilic Layers* (Ref. [1]), p. 118; more recent results can be found in D. Roux, F. Nallet, E. Freyssingeas, G. Porte, P. Bassereau, M. Skouri, and J. Marignan, Europhys. Lett. **17**, 575 (1992).